TFIIA–TAF regulatory interplay: NMR evidence for overlapping binding sites on TBP

Stefan Bagby[a], Tapas K. Mal[a], Dingjiang Liu[a], Elaine Raddatz[a], Yoshihiro Nakatani[b], Mitsuhiko Ikura[a],*

[a]*Division of Molecular and Structural Biology, Ontario Cancer Institute, and Department of Medical Biophysics, University of Toronto, 610 University Avenue, Toronto, Ont. M5G 2M9, Canada*
[b]*Laboratory of Molecular Growth Regulation, National Institute of Child Health and Human Development, National Institutes of Health, Bethesda, MD 20892, USA*

Abstract TATA box binding protein (TBP)–promoter interaction nucleates assembly of the RNA polymerase II transcription initiation complex. Transcription factor IIA (TFIIA) stabilizes the TBP–promoter complex whereas the N-terminal domain of the largest TAF_{II} inhibits TBP–promoter interaction. We have mapped the interaction sites on TBP of *Drosophila* $TAF_{II}230$ and yeast TFIIA (comprising two subunits, TOA1 and TOA2), using nuclear magnetic resonance (NMR), and also report structural evidence that subdomain II of the $TAF_{II}230$ N-terminal inhibitory domain and TFIIA have overlapping binding sites on the convex surface of TBP. Together with previous mutational and biochemical data, our NMR results indicate that subdomain II augments subdomain I-mediated inhibition of TBP function by blocking TBP-TFIIA interaction.
© 2000 Federation of European Biochemical Societies.

Key words: TATA box binding protein; TBP-associated factor; Transcription factor IIA; Nuclear magnetic resonance; Heteronuclear single quantum coherence

1. Introduction

Initiation of transcription by RNA polymerase II requires the auxiliary transcription factors (TF) IIA, TFIIB, TFIID, TFIIE, TFIIF and TFIIH [1]. The TATA box binding protein (TBP) subunit of TFIID nucleates assembly of the RNA polymerase II complex through its sequence-specific recognition and binding of the TATA element of the core promoter. TFIIA stimulates and stabilizes TBP binding to TATA-containing DNA [2] by direct interaction with TBP and DNA [3,4]. In the step-wise model of transcription complex assembly based on in vitro studies [5,6], subsequent ordered assembly of TFIIB, the RNA polymerase II–TFIIF complex and TFIIE and TFIIH completes transcription initiation complex formation.

Structural studies of the RNA polymerase II auxiliary factors have contributed greatly to our understanding of the macromolecular interactions supporting assembly of the RNA polymerase II transcription initiation complex. The crystal structures of TBP [7,8] and the TBP–TATA box complex [9,10] revealed a large concave undersurface on TBP

formed by a curved, eight-stranded, antiparallel β-sheet which makes minor groove and phosphate-ribose contacts and induces partial unwinding of the eight base pair TATA element. In the TFIIA–TBP–TATA ternary complex crystal structure [3,4], the principal TFIIA–TBP interface involves the outer β-strand of TBP leading to the N-terminal stirrup of TBP. Mutagenesis and biochemical studies [11–15] have indicated that there is a direct interaction of helix 2 of TBP with TFIIA. This interaction was not observed, however, in the TFIIA–TBP–TATA crystal structures [3,4].

In addition to TBP, TFIID contains numerous other phylogenetically conserved subunits termed the TBP-associated factors (TAF_{II}s) [16], which modulate the promoter recognition and transcriptional activities of TBP [17]. For example, in yeast (y), *Drosophila* (d) and human (h), the largest TAF_{II} possesses an N-terminal inhibitory domain (NID) that blocks TBP–TATA binding through direct interaction with TBP [18–21]. The NID can be dissected into two subdomains, I and II (residues 2–81 and 82–156 of $dTAF_{II}230$) (Fig. 1A). We have previously determined the three-dimensional structure of the complex between TBP and $dTAF_{II}230$ subdomain I, revealing an elegant mechanism for autoinhibition in which subdomain I occupies the concave DNA binding surface of TBP and undergoes an extensive degree of induced folding to mimic the partially unwound structure of a TBP-bound TATA element [22].

TFIIA and TAF_{II}s are involved in a dynamic interplay to regulate binding of TFIID to promoter DNA [15,23–29]. In order to extend our understanding of the interplay between TBP, inhibitory $dTAF_{II}230$ and stimulatory TFIIA, and to account for the discrepancy between biochemical and crystallographic studies concerning the role of TBP helix 2 in binding TFIIA, we have measured peak attenuation and chemical shift changes in nuclear magnetic resonance (NMR) spectra to map the binding sites on yTBP of $dTAF_{II}230$ NID subdomain II (Fig. 1B) and yTFIIA (a heterodimer of 32 kDa TOA1 and 13.5 kDa TOA2) [30,31]. A study using peptides reported an interaction between the helix 2 region of hTBP and the fragment comprising residues 281–301 of the β subunit of hTFIIA [32]. The present study was carried out with full-length yTFIIA, however, and therefore presents a more complete picture of TFIIA–TBP interactions. Our report also provides structural evidence that TFIIA and $dTAF_{II}230$ subdomain II have overlapping binding sites on TBP, including helix 2. The dynamics of both TFIIA–TBP and $dTAF_{II}230$ subdomain II–TBP interactions, evidenced by extensive broadening of TBP

*Corresponding author. Fax: (1)-416-946 2055/6529.
E-mail: mikura@oci.utoronto.ca

NMR signals in the binding region and undefined electron density in a TFIIA segment important for TBP binding [4,33], hinder more detailed structural analysis. The high molecular weight ($\sim$74 kDa) of the TBP–dTAF$_{II}$230(11–77)–TFIIA complex is also a major hindrance to detailed structural study by NMR.

2. Materials and methods

2.1. Protein expression and purification

The protocols for obtaining the C-terminal core domain (residues 49–240) of *Saccharomyces cerevisiae* TBP (MW 21.3 kDa) and *Drosophila* TAF$_{II}$230(11–77) have been described previously [22]. dTAF$_{II}$230(1–156) was purified in essentially the same manner as dTAF$_{II}$230(11–77) [22]. Since dTAF$_{II}$230(1–156) is more acidic than dTAF$_{II}$230(11–77), however, the TBP–dTAF$_{II}$230(1–156) complex was separated from its unbound individual components by gel filtration instead of cation exchange. *S. cerevisiae* TFIIA (full length TOA1 and TOA2 subunits, producing a heterodimer of total MW 45.5 kDa) was expressed and purified as described previously [15]. Separation of complexed from non-complexed TFIIA subunits and further purification was achieved by gel filtration using Superdex 75 (Pharmacia).

2.2. NMR data collection and analysis

^{1}H-^{15}N heteronuclear single quantum coherence (HSQC) spectra were recorded using a 500 MHz Varian INOVA spectrometer. All spectra were recorded at 25°C with 144 complex t_1 increments of 1000 complex data points and 160 transients except in the second and third points of the TFIIA titration where 216 and 232 transients were recorded. Spectral widths were 32.7 ppm and 16.0 ppm for the ^{15}N (F$_1$) and ^{1}H (F$_2$) dimensions. NMR samples containing ^{15}N TBP in complex with either unlabelled dTAF$_{II}$230(11–77) or unlabelled dTAF$_{II}$230(1–156) were prepared as described previously [22]. ^{1}H-^{15}N HSQC peak intensities were obtained using Pipp [34] and normalized by the intensity of a peak from a side chain NH$_2$ group that is expected to be unstructured in all samples.

The TFIIA titration was carried out as follows: a ^{15}N TBP–dTAF$_{II}$230(11–77) NMR sample of about 0.5–0.7 mM was made and its ^{1}H-^{15}N HSQC spectrum was recorded to verify the equivalence of the sample to those used in our previous studies [22]. This NMR sample was diluted from 0.5 ml to 2.5 ml using NMR sample buffer [22] and TFIIA was then added dropwise to it. The sample was then concentrated to 0.5 ml with a final TFIIA concentration of approximately 0.11 mM. After recording a ^{1}H-^{15}N HSQC spectrum, a second addition of TFIIA was carried out in the same manner as the first, giving a final TFIIA concentration of approximately 0.19 mM. The third addition of TFIIA gave a final TFIIA concentration of approximately 0.28 mM.

3. Results

The dTAF$_{II}$230 subdomain II binding site on TBP was defined by comparing the ^{1}H-^{15}N HSQC spectrum of uniformly ^{15}N-labelled TBP in the TBP–dTAF$_{II}$230(1–156) complex with the corresponding spectrum of TBP in the dTAF$_{II}$230(11–77) complex (Fig. 2A,B). Any noteworthy differences between the two spectra were due to the presence of subdomain II, residues 82–156, of dTAF$_{II}$230. The most obvious difference noticed was the overall increase in linewidth of NMR signals for the TBP–dTAF$_{II}$230(1–156) complex (data not shown), due to the increase in molecular weight of the complex from about 28.5 kDa to 38 kDa. The selective further broadening of certain TBP peaks illustrated in Fig. 2 arose from intermediate timescale exchange between TBP-bound and unbound states of dTAF$_{II}$230 subdomain II. This contrasts with the tight TBP–dTAF$_{II}$230 subdomain I interaction (K_d in the low nM range) which is dominated by hydrophobic contacts and exhibits slow exchange between bound and unbound forms [22]. Thus, the two subdomains

of dTAF$_{II}$230 simultaneously bind TBP with different timescales of chemical exchange between bound and unbound forms. The TBP–dTAF$_{II}$230 subdomain II interaction is most probably dominated by electrostatic contacts given the high proportion of acidic amino acids in subdomain II (33% compared to 21% in subdomain I of dTAF$_{II}$230; Fig. 1B), the amphipathic, basic nature of the C-terminal half of TBP helix 2 and that mutation studies indicate that acidic residues in yTAF$_{II}$145 subdomain II contribute to the binding to TBP [15]. A titration of TBP with dTAF$_{II}$230(1–156) could not be performed because free TBP is unstable and precipitates readily under the buffer conditions and protein concentrations used for the TBP–TAF$_{II}$ NMR samples, which are made by mixing dilute TBP and TAF$_{II}$.

The TFIIA binding site on TBP was mapped similarly, except that the ^{15}N TBP–dTAF$_{II}$230(11–77) complex was titrated with unlabelled TFIIA. A ^{1}H-^{15}N HSQC spectrum of TBP was recorded at each titration point (Fig. 2A,C). Selective effects were observed upon the first and second additions of TFIIA, and most TBP HSQC peaks were broadened to or close to the level of the spectral noise after the third addition of TFIIA. The TBP–dTAF$_{II}$230(11–77) complex provides an excellent platform for investigating the interaction of TBP with TFIIA in solution: the TBP–dTAF$_{II}$230(11–77) complex structurally resembles the TBP–DNA complex [22], the sample is sufficiently stable for detailed NMR studies and can be routinely generated.
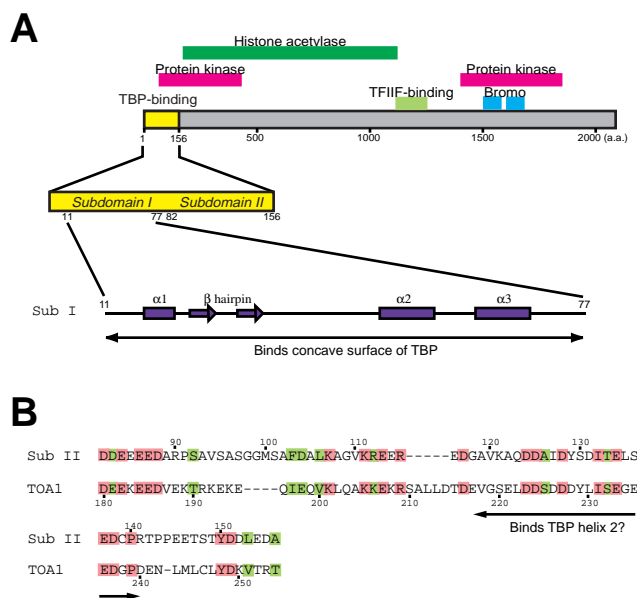
dTAF$_{II}$230 subdomain II and TFIIA caused attenuation

Fig. 1. Features of dTAF$_{II}$230 and TOA1. A: Schematic depiction of full-length dTAF$_{II}$230. Proposed domain locations and functions are shown. The N-terminal TBP inhibitory domain is highlighted in yellow and the sequence locations of subdomains I and II are indicated. The secondary structure of subdomain I is taken from a previous structural study [22]. B: Sequence alignment of dTAF$_{II}$230 subdomain II and TOA1 residues 180–254. Identical amino acids are highlighted in pink and conservatively substituted amino acids in green. The region of TOA1 (residues 217–240) essential for formation of stable TFIIA complexes with TBP and TBP–DNA [33] is marked with a double-headed arrow and its putative interaction with TBP helix 2 is indicated. Sequences were aligned using CLUSTAL W [40].
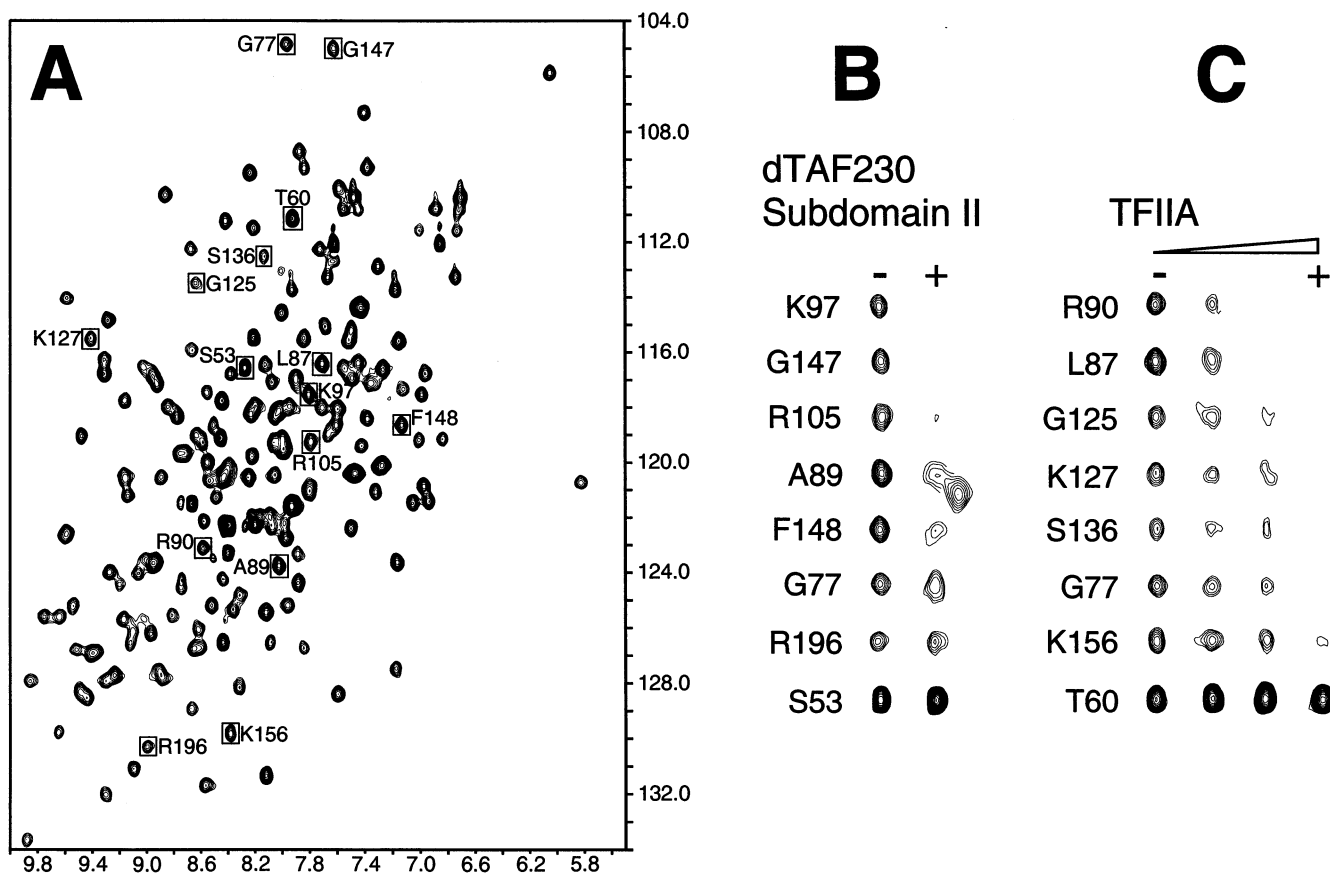
Fig. 2. dTAF$_{II}$230 subdomain II and TFIIA interaction with TBP. A: ^{1}H-^{15}N HSQC spectrum of ^{15}N-labelled TBP in complex with unlabelled dTAF$_{II}$230(11–77). The ^{15}N TBP–dTAF$_{II}$230(11–77) complex spectrum was used as reference for mapping the binding sites on TBP of dTAF$_{II}$230 subdomain II (B) and TFIIA (C). The peaks shown in B and C are boxed and labelled with the relevant TBP amino acid residue name and sequence position. B: Examples of the selective TBP peak attenuation due to binding of dTAF$_{II}$230 subdomain II (residues 82–156) to TBP. Each row contains a TBP amino acid residue name and sequence position, the peak due to that residue from the spectrum shown in A (− column) followed by the corresponding peak from the ^{1}H-^{15}N HSQC spectrum of ^{15}N-labelled TBP in complex with unlabelled dTAF$_{II}$230(1–156) (+ column). A blank in the + column indicates that the peak has been broadened to the level of the spectral noise. The peaks are listed in decreasing order of subdomain II-induced attenuation. For example, the Lys-97 peak is broadened to the level of the spectral noise, the Arg-196 peak is slightly attenuated and the Ser-53 peak is not attenuated at all. C: Examples of the selective TBP peak attenuation due to binding of TFIIA to TBP in a three-point titration of TFIIA into a sample of ^{15}N-labelled TBP complexed with unlabelled dTAF$_{II}$230(11–77). Each row contains a TBP amino acid residue name and sequence position, the peak due to that residue from the spectrum shown in A followed by the corresponding peak from each of the ^{1}H-^{15}N HSQC spectra recorded at the three points in the TFIIA titration with successively greater levels of TFIIA. The peaks are listed in decreasing order of TFIIA-induced attenuation.

(Fig. 2B,C) and/or chemical shift changes of the backbone amide peaks of numerous residues in the N-terminal α/β-repeat motif of TBP, within the stretches Leu-87 to Glu-108 and Lys-133 to Phe-152 (dTAF$_{II}$230 subdomain II; Fig. 3), and Thr-73 to Glu-108 and Gly-125 to Lys-145 (TFIIA; Fig. 4). Since a significant chemical shift change or peak attenuation indicates that the residue concerned is located at or close to the intermolecular interface, these data indicate that dTAF$_{II}$230 subdomain II and TFIIA have overlapping binding sites on the TBP surface localized to the N-terminal α/β-repeat motif. Leu-87 to Glu-108 includes the C-terminal part of helix 1 (residues 82–89) and the N-terminal stirrup, and Lys-133 to Phe-152 includes helix 2 (residues 129–146) and the subsequent loop on the convex upper TBP surface (Fig. 3A). TFIIA exerted significant effects also on TBP residues preceding Leu-87, including the strand and loop leading to helix 1 (Fig. 4A).

The strongest peak attenuation by TFIIA occurred at TBP residues Leu-87, Arg-90 and Arg-141. Leu-87 and Arg-90 lie in and just C-terminal to helix 1, while Arg-141 lies in helix 2 on the convex upper surface of TBP (Fig. 4). Within the fragment from Thr-73 to Glu-108, TFIIA addition also significantly affected TBP residues Asn-91, Glu-93 and Asn-95 and others in the vicinities of Lys-83, Arg-105 and Arg-107. These effects correlate well with the crystal structure of the yTFIIA–yTBP–DNA complex [3,4], wherein the predominant TFIIA–TBP binding interface involves the β-strand (amino acids 91, 92 and 94) leading to the N-terminal TBP stirrup.

Generally, dTAF$_{II}$230 subdomain II induced little or no change in the chemical shifts of residues making up the concave DNA binding surface of TBP, indicating that dTAF$_{II}$230 subdomain II does not exert a significant widespread effect on the interaction between TBP and dTAF$_{II}$230 subdomain I. Met-104 and Ile-106 did, however, undergo relatively large chemical shift changes, perhaps reflecting a local structural perturbation at an edge of the concave TBP β-sheet (Fig. 3A). The path of the N-terminal part of subdomain II inferred from these and other effects in the vicinity of the TBP N-
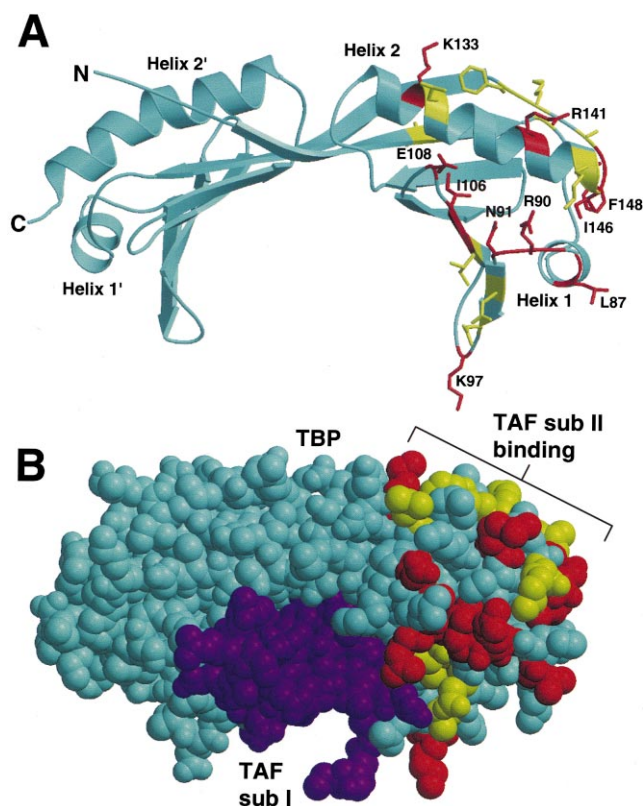
Fig. 3. dTAF$_{II}$230 subdomain II interaction with TBP. A: Ribbon representation of TBP taken from the structure of the complex between TBP and dTAF$_{II}$230 subdomain I [22]. TBP residues most affected by binding of dTAF$_{II}$230 subdomain II, as determined by NMR, are highlighted in red (strong effect) and yellow (medium effect) and their sidechains are shown. B: Space-filling representation of the complex between TBP (cyan) and dTAF$_{II}$230(11–77) (dark violet). The residues most affected by binding of dTAF$_{II}$230 subdomain II are highlighted in red (strong effect) and yellow (medium effect) as in A. The inferred binding of dTAF$_{II}$230 subdomain II to TBP helix 2 is indicated. This figure was created using MOL-SCRIPT [41].

terminal stirrup (Fig. 3) is consistent with the proximal location of the C-terminus of subdomain I observed in the structure of the TBP–dTAF$_{II}$230 subdomain I complex [22].

dTAF$_{II}$230 subdomain II and TFIIA effects on several TBP residues between Thr-73 and Glu-108 and in helix 2 could not be ascribed due to peak overlap or absence from the TBP–dTAF$_{II}$230(11–77) spectrum. These included Ala-92 and Tyr-94 and helix 2 basic residues Arg-137 and Lys-138; Lys-138 was part of the (Lys-133, 138, 145-Glu) mutation that weakened TBP interaction with yTAF$_{II}$145 NID, and the (Lys-138-Thr, Tyr-139-Ala) and (Lys-133,138,145-Glu) mutations that abolished TBP–DNA interaction with TFIIA [13,15].

4. Discussion

Structural knowledge of the interactions leading to repression, derepression and net activation of transcription is limited. TFIID–promoter interaction is a key process for transcriptional regulation that can be rate limiting for transcription in vivo [35–38]. Accordingly, numerous activators and repressors of transcription influence this step in RNA polymerase II complex assembly. For example, the N-terminal domain of the largest TAF$_{II}$ of yeast, *Drosophila* and human

TFIID strongly interacts with TBP and inhibits TBP function [15,19,20,29,39]. Evidence from biochemical experiments suggests that TFIIA supports activated transcription at least in part by competing for binding to TBP with the NID of the largest TAF$_{II}$ [15,29]. Our NMR-based observation that yTFIIA and dTAF$_{II}$230 subdomain II have overlapping binding sites on TBP, including helix 1, the subsequent loop to strand 1, the N-terminal stirrup, strand 2 and notably helix 2 on the convex upper TBP surface (Figs. 3 and 4), provides structural evidence in support of the biochemical evidence [15,29] that TFIIA and subdomain II compete for access to TBP. This indicates that subdomain II augments the inhibitory effect of subdomain I by hindering the TBP–TFIIA interaction that stabilizes the TBP–DNA complex and supports transcriptional activation.

The NMR data indicate that both TFIIA and dTAF$_{II}$230 subdomain II contact helix 2 on the convex upper surface of
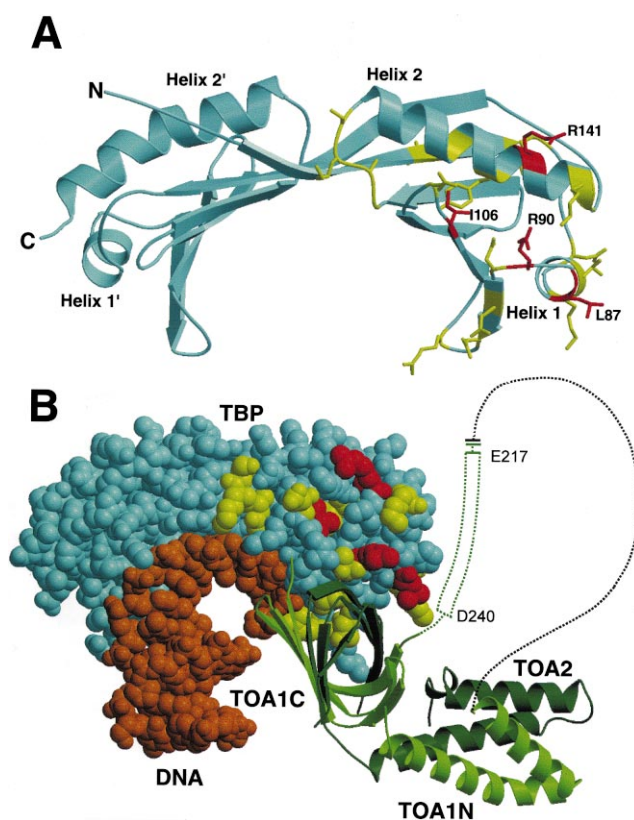

Fig. 4. TFIIA interaction with TBP. A: Ribbon representation of TBP taken from the structure of the complex between TBP and dTAF$_{II}$230 subdomain I [22]. TBP residues most affected by binding of TFIIA, as determined by NMR, are highlighted in red (strong effect) and yellow (medium effect) and their sidechains are shown. B: Space-filling representation of the yTFIIA–yTBP–DNA complex taken from the ternary complex crystal structure [4]. TBP is shown in cyan, DNA in orange and the TOA1 and TOA2 subunits of yTFIIA as light and dark green ribbons. TBP residues affected by TFIIA binding in solution are shown in red (strong effect) and yellow (medium effect) as in A. Full-length TOA1 and TOA2 were used in this NMR study. TOA1 residues 210–240, not well defined in the electron density map [4], are represented by a light green dashed line with residues 217–240, required for stable TFIIA–TBP or TFIIA–TBP–DNA complex formation [33], highlighted. TOA1 used for crystallization contained a large central deletion between residues 55 and 207 [4] or between 95 and 209 [3]. This deleted region is represented by a black dashed line. This figure was created using MOLSCRIPT [41].

TBP, probably primarily through basic TBP residues such as Lys-138 (amide peak absent from TBP HSQC spectrum), Arg-141 and Lys-145 (amide peaks attenuated by TFIIA). This result is consistent with previous biochemical in vitro results [11,12,14] and genetic in vivo results [13] which suggested that TBP helix 2 is important for interaction with TFIIA. However, no TBP helix 2–TFIIA contact was observed in the yTFIIA–yTBP–DNA complex crystal structures [3,4]. Geiger et al. [3] suggested that the human and yeast TBP–TFIIA complexes differ and proposed that only human complex includes an interaction between TFIIA and TBP helix 2. Alternatively, residues 210–240 of the larger TFIIA subunit, TOA1 (Fig. 4B), poorly defined in the electron density map, may form a 'long shoelace' that contacts TBP helix 2 and subsequently wraps around TBP to contact the side of TBP helix 1 [4]. This possibility is supported by several observations, including: TOA1 residues 217–240 are necessary for the formation of stable TFIIA–TBP and TFIIA–TBP–DNA complexes [33]; the proposed path has several basic TBP residues to complement the highly acidic TOA1 shoelace (sequence shown in Fig. 1B); and the yTBP helix 2 double mutation Lys-138-Thr, Tyr-139-Ala weakens or abolishes yTBP–yTFIIA interaction in vitro and in vivo [13]. By indicating that yTFIIA does contact TBP helix 2, our results are consistent with these observations. In further support of the proposed [4] path of TOA1 residues 210–240, TFIIA affects TBP helix 1 residues (Fig. 4A,B), indicating that yTFIIA also contacts TBP helix 1. The sequence similarity of subdomain II and TOA1 residues 210–240 (Fig. 1B), particularly the acidic character, is consistent with similar paths along the TBP surface. In support of the proposal by Geiger et al. [3], some of the previous biochemical results [11] indicate that hTFIIA may make more extensive contacts than yTFIIA with TBP helix 2, although confirmation requires structural analysis of a human TFIIA–TBP–DNA complex.

The lack of TFIIA–TBP helix 2 contacts in the ternary complex crystal structures may arise from the large central deletion (residues 95–209 or 55–207) in the TOA1 subunit used for crystallization [3,4], resulting in two polypeptides (TOA1N and TOA1C in Fig. 4B). This may affect the conformation of the fragment (residues 217–240) required for formation of stable TFIIA complexes with TBP and TBP–DNA [33], since this fragment is close to the N-terminus of TOA1C. It might conversely be argued that the TBP–TFIIA contacts determined by NMR, using TBP–dTAF$_{II}$230(11–77) instead of TBP–TATA as a platform, do not necessarily reflect the TBP–TFIIA contacts in a TFIIA–TBP–TATA complex. The TFIIA-induced changes in TBP NMR spectra discussed above, however, indicate that TBP–TFIIA contacts in the TBP–dTAF$_{II}$230(11–77) complex correspond to those observed in the TFIIA–TBP–TATA crystal structures, with the major exception of the helix 1 and helix 2 contacts.

The results of this and other studies [15,21,22] indicate that VP16 activation domain and yTAF$_{II}$145/dTAF$_{II}$230/hTAF$_{II}$250 subdomain I compete for binding to the concave undersurface of TBP, whereas TFIIA and yTAF$_{II}$145/dTAF$_{II}$230/hTAF$_{II}$250 subdomain II compete for binding to the convex upper surface of TBP. These observations lead to an appealing model in which the repressive TBP–yTAF$_{II}$145/dTAF$_{II}$230/hTAF$_{II}$250 interaction is counteracted by TFIIA in concert with one or more activators, the latter to relieve the inhibitory TAF$_{II}$ interaction on the TBP concave surface, TFIIA to relieve the inhibitory TAF$_{II}$ interaction on the convex TBP surface. It remains unclear how the DNA binding surface of TBP is subsequently released to permit the slow association of TBP with DNA without allowing the presumably more facile inhibitory TBP–TAF$_{II}$ interaction to re-occur.

References

[1] Hampsey, M. (1998) Microbiol. Mol. Biol. Rev. 62, 465–503.
[2] Imbalzano, A.N., Zaret, K.S. and Kingston, R.E. (1994) J. Biol. Chem. 269, 8280–8286.
[3] Geiger, J.H., Hahn, S., Lee, S. and Sigler, P.B. (1996) Science 272, 830–836.
[4] Tan, S., Hunziker, Y., Sargent, D.F. and Richmond, T.F. (1996) Nature 381, 127–134.
[5] Buratowski, S., Hahn, S., Guarente, L. and Sharp, P.A. (1989) Cell 56, 549–561.
[6] Flores, O., Lu, H. and Reinberg, D. (1992) J. Biol. Chem. 267, 2786–2793.
[7] Nikolov, D.B., Hu, S.H., Lin, J., Gasch, A., Hoffmann, A., Horikoshi, M., Chua, N.H., Roeder, R.G. and Burley, S.K. (1992) Nature 360, 40–46.
[8] Chasman, D.I., Flaherty, K.M., Sharp, P.A. and Kornberg, R.D. (1993) Proc. Natl. Acad. Sci. USA 90, 8174–8178.
[9] Kim, Y., Geiger, J.H., Hahn, S. and Sigler, P.B. (1993) Nature 365, 512–520.
[10] Kim, J.L., Nikolov, D.B. and Burley, S.K. (1993) Nature 365, 520–527.
[11] Buratowski, S. and Zhou, H. (1992) Science 255, 1130–1132.
[12] Lee, D.K., DeJong, J., Hashimoto, S., Horikoshi, M. and Roeder, R.G. (1992) Mol. Cell. Biol. 12, 5189–5196.
[13] Stargell, L.A. and Struhl, K. (1995) Science 269, 75–78.
[14] Tang, H., Sun, X., Reinberg, D. and Ebright, R.H. (1996) Proc. Natl. Acad. Sci. USA 93, 1119–1124.
[15] Kokubo, T., Swanson, M.J., Nishikawa, J.-I., Hinnebusch, A.G. and Nakatani, Y. (1998) Mol. Cell Biol. 18, 1003–1012.
[16] Burley, S.K. and Roeder, R.G. (1996) Annu. Rev. Biochem. 65, 769–799.
[17] Verrijzer, C.P. and Tjian, R. (1996) Trends Biochem. Sci. 21, 338–342.
[18] Kokubo, T., Takada, R., Yamashita, S., Gong, D.W., Roeder, R.G., Horikoshi, M. and Nakatani, Y. (1993) J. Biol. Chem. 268, 17554–17558.
[19] Kokubo, T., Yamashita, S., Horikoshi, M., Roeder, R.G. and Nakatani, Y. (1994) Proc. Natl. Acad. Sci. USA 91, 3520–3524.
[20] Bai, Y., Perez, G.M., Beechem, J.M. and Weil, P.A. (1997) Mol. Cell. Biol. 17, 3081–3093.
[21] Nishikawa, J., Kokubo, T., Horikoshi, M., Roeder, R.G. and Nakatani, Y. (1997) Proc. Natl. Acad. Sci. USA 94, 85–90.
[22] Liu, D., Ishima, R., Tong, K.I., Bagby, S., Kokubo, T., Muhandiram, R., Kay, L.E., Nakatani, Y. and Ikura, M. (1998) Cell 94, 573–583.
[23] Lieberman, P.M. and Berk, A.J. (1994) Genes Dev. 8, 995–1006.
[24] Ozer, J., Moore, P.A., Bolden, A.H., Lee, A., Rosen, C.A. and Lieberman, P.M. (1994) Genes Dev. 8, 2324–2335.
[25] Chi, T., Lieberman, P., Ellwood, K. and Carey, M. (1995) Nature 377, 254–257.
[26] Chi, T. and Carey, M. (1996) Genes Dev. 10, 2540–2550.
[27] Lagrange, T., Kim, T.K., Orphanides, G., Ebright, Y.W., Ebright, R.H. and Reinberg, D. (1996) Proc. Natl. Acad. Sci. USA 93, 10620–10625.
[28] Oelgeschlager, T., Chiang, C.M. and Roeder, R.G. (1996) Nature 382, 735–738.
[29] Ozer, J., Mitsouras, K., Zerby, D., Carey, M. and Lieberman, P.M. (1998) J. Biol. Chem. 273, 14293–14300.

[30] Ranish, J.A. and Hahn, S. (1991) J. Biol. Chem. 266, 19320–19327.

[31] Ranish, J.A., Lane, W.S. and Hahn, S. (1992) Science 255, 1127–1129.

[32] Ramboarina, S., Morellet, N., Petitjean, P., Roques, B.P. and Fournie-Zaluski, M.-C. (1998) Protein Eng. 11, 729–738.

[33] Kang, J.J., Auble, D.T., Ranish, J.A. and Hahn, S. (1995) Mol. Cell. Biol. 15, 1234–1243.

[34] Garrett, D.S., Powers, R., Gronenborn, A.M. and Clore, G.M. (1991) J. Magn. Reson. 95, 214–220.

[35] Colgan, J. and Manley, J.L. (1992) Genes Dev. 6, 304–315.

[36] Klein, C. and Struhl, K. (1994) Science 266, 280–282.

[37] Chatterjee, S. and Struhl, K. (1995) Nature 374, 820–822.

[38] Klages, N. and Strubin, M. (1995) Nature 374, 822–823.

[39] Kokubo, T., Gong, D.W., Yamashita, S., Horikoshi, M., Roeder, R.G. and Nakatani, Y. (1993) Genes Dev. 7, 1033–1046.

[40] Thompson, J.D., Higgins, D.G. and Gibson, T.J. (1994) Nucleic Acids Res. 22, 4673–4680.

[41] Kraulis, P. (1991) J. Appl. Crystallogr. 24, 946–950.